

Citation:

Hodder, A.P.W.; Naish, T.R.; Lowe, D.J. 1996. Towards an understanding of thermodynamic and kinetic controls on the formation of clay minerals from volcanic glass under various environmental conditions. Pp. 1-11 (Chapter 1) in Pandalai, S. G. (Ed) *Recent Research Developments in Chemical Geology*. Research Signpost, Trivandrum.

Recent Res. Devel. in Chemical Geol., 1 (1996)

Towards an understanding of thermodynamic and kinetic controls on the formation of clay minerals from volcanic glass under various environmental conditions

A.P.W. Hodder, T.R. Naish and D.J. Lowe

Department of Earth Sciences, University of Waikato, Private Bag 3105, Hamilton, New Zealand

Thermodynamic stability diagrams based on a topological procedure constrained by thermodynamic data for idealised smectites and imogolite indicate that imogolite is the favoured alteration product of rhyolitic volcanic glass in both the soil and nearshore marine environments. However, smectites are observed in young nearshore marine sediments, suggesting a rapid alteration. The rate of formation of clay minerals has been previously demonstrated to be a function of their equilibrium constant (K) and the reaction activity quotient (Q) - effectively the divergence from equilibrium. Extending this treatment to include the process of glass dissolution (θ) as a prelude to clay mineral formation (ϕ), the rate of clay mineral formation is demonstrated to be a function of the parameter:

$$k_+(1-Q_\theta/K_\theta) - k'_+(1-Q_\phi/K_\phi)$$

Where k_+ and k'_+ are the rate constants of dissolution for glass and clay respectively. The values of Q_θ/K_θ are such that in general, the rate determining step is determined by Q_ϕ/K_ϕ .

Based on this approach, the rate of formation of smectite is fast in silica saturated interstitial waters in the nearshore marine environment, perhaps a thousand times faster than the formation of imogolite or halloysite in soil waters.

INTRODUCTION

The weathering of rhyolitic volcanic glass, chiefly from tephric materials, to form clay minerals has been extensively studied (e.g.1; 2; 3; 4; 5). Clay mineralogists and pedologists have been principally concerned about the structure and composition of the derived clay minerals, and their effects on soils or paleosols, but there has been comparatively little consideration of the thermodynamics and kinetics

behind these processes. Ruxton (6) recognised that the formation of clay minerals from glass was essentially a first-order process: that the proportion of clay minerals (P_c) was related to the initial proportion of glass (P_g^0) by a relationship of the form.

$$P_c/P_g^0 = \exp(-k_1 t) \quad (1)$$

where k_1 is the rate constant for the process and t is the time for weathering.

On a rather shorter time-scale, the development of hydration rinds on obsidian artefacts (e.g., 7; 8; 9) and studies on the dissolution of glass in the laboratory suggested that this was a diffusion controlled process (10; 11), for which a typical expression for the change in concentration (C) with time (t) is of the form:

$$C = C_0 k_p t^{1/2} \quad (2)$$

where C_0 is the concentration initially and k_p is the so-called "parabolic rate constant". For young tephra deposits, this diffusion process may be an important part of the total weathering process. A model coupling the first-order and diffusional process represented by equations (1) and (2) was developed (12) and then applied to glasses weathering to allophane (Si-rich allophane with Al:Si ratio of 1:1 as in halloysite), imogolite (Al-rich [proto-imogolite] allophane with Al:Si ratio of 2:1), or halloysite in the soil-forming environment (13). In the marine environment bentonite has long been recognised as an alteration product of volcanic glass (e.g., 14). Most studies of bentonites imply that because their formation has been from volcanic ash or tuff deposits in deep-sea sediments of at least Pleistocene age (e.g., 15; 16; 17; 18; 19), factors such as time, burial and temperature are important to bentonite formation. "Bentonite" has been used quite generally to describe the alteration products, which include smectite clay minerals and zeolites (20). More recently late Holocene estuarine sediments adjacent to a volcanic terrain (Firth of Thames, New Zealand) have been recognised as containing large

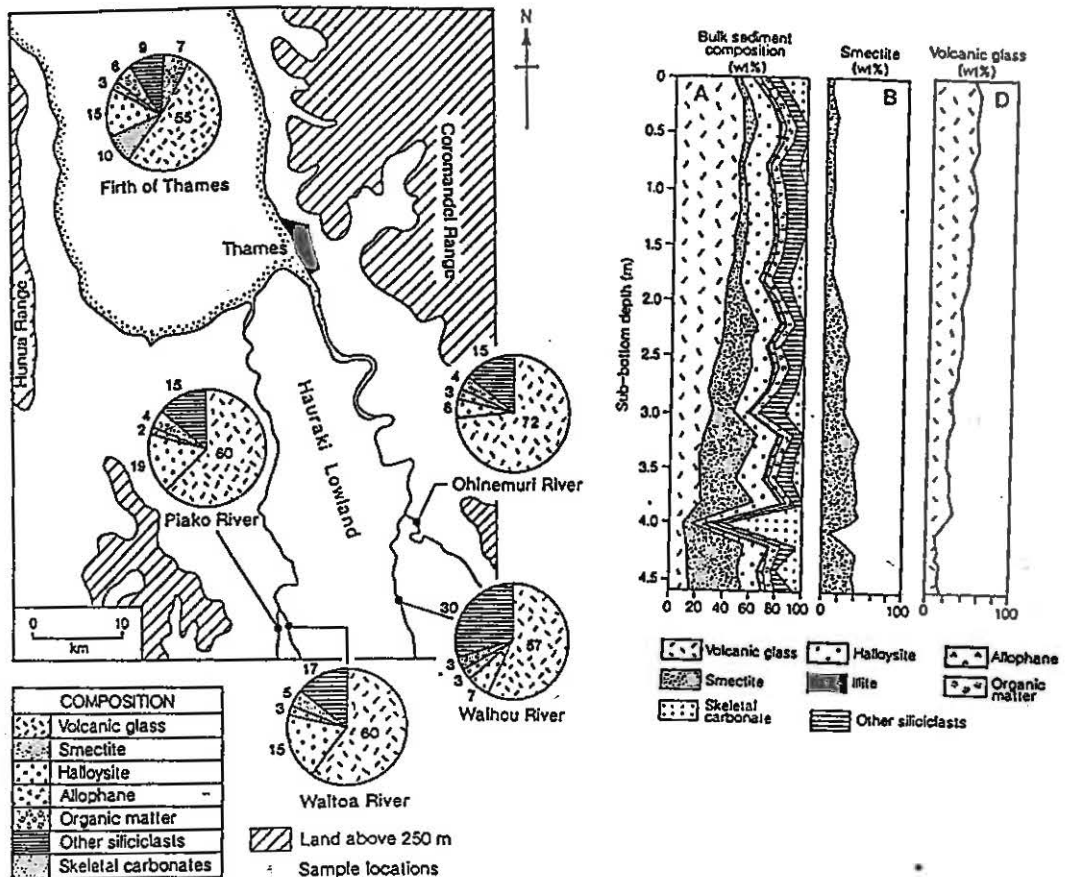


FIG 1. A. Composition of sediments in rivers entering the Firth of Thames, New Zealand, and surficial sediments of the firth. B. Compositional logs for a representative core in the Firth of Thames (21). (Types of allophane are not distinguished in the core logs).

amounts of smectite (21). The mineralogy of the streams draining the region and entering the Firth does not include smectite, but does include abundant volcanic glass (Fig. 1). Naish (21) considered it likely that the smectite was forming from the volcanic glass under early diagenetic conditions in the Firth, and Hodder *et al.* (22) proposed a two-stage model for the kinetics of smectite formation from detrital volcanic glass analogous to that previously developed for imogolite formation from glass in tephra-derived paleosols.

The question remains: what are the environmental conditions that enable smectite to be

formed in the nearshore marine environment, but imogolite (or allophane or halloysite) in the soil-forming environment? By the use of thermodynamic stability diagrams and the recognition that relative mineral solubilities may be proxies for rate constants for mineral dissolution or precipitation, this paper shows that high silica concentrations in solutions of high ionic strength are required to precipitate smectite, but that the solution needs to have only a high silica content to ensure formation of imogolite.

THERMODYNAMIC STABILITY DIAGRAMS

The representation of thermodynamic stability for clay minerals formed as a result of 'weathering' (in

the soil-forming environment) or 'diagenesis' (in the nearshore marine environment) of glass is made more difficult by the absence of free energy data for the glass and for allophane. To some extent this difficulty can be reduced by a topological approach (23). For this approach, only the compositions of the minerals are required to be known. For two minerals to be in equilibrium, the compositions on an appropriate plot are joined (see Fig. 2). Such tie-lines may not intersect, and the tie-lines are at right angles to the line defining equilibrium between the minerals on the thermodynamic stability diagram. Such compositional diagrams and their derived stability diagrams are shown for the $\text{Na}_2\text{O}-\text{SiO}_2-\text{Al}_2\text{O}_3-\text{H}_2\text{O}$ and $\text{CaO}-\text{SiO}_2-\text{Al}_2\text{O}_3-\text{H}_2\text{O}$ systems on Figs 2 and 3, respectively. Data for the free energies of the clay minerals enable these diagrams to be better constrained. For this purpose the Gibbs standard free energy of formation of Si-rich allophane is taken as that of halloysite, the Gibbs standard free energy of formation for smectite clay minerals is taken as that for idealised N and Ca-beidellites (23), and the value for imogolite is as calculated by Percival (24).

The limiting positions of the stability lines are shown (broken lines on lower part of Fig. 2) as defining glass in equilibrium with imogolite and halloysite only, or with smectite and halloysite only. An intermediate position (solid line) allows equilibrium between glass and all the clay minerals.

Also shown on these diagrams are the compositions of seawater and the range of compositions of soil water from topsoils formed from rhyolitic tephra (volcanic ash) (25). These soil-water compositions lie mainly within the calculated stability field for imogolite but some are in the halloysite stability field. This is in accord with the observations (26) of low soil solution silicon is present in soils where proto-imogolite allophane is predominant, but halloysite predominates in soils of relatively high solution silicon. The values for seawater are close to the zeolite-imogolite boundary, well distant from the smectite stability field. If smectite is to be formed from rhyolitic glass in the marine environment, either the solution chemistry has to change during early diagenesis or the process is kinetically controlled, or both.

A decrease in the $(\log a_{\text{Na}^+} + \text{pH})$ or $\log(a_{\text{Ca}^{2+}} + 2\text{pH})$ values could reasonably occur with the reduction of pH, reasonably expected during diagenesis by the reduction of seawater sulfate and in response to the bacterially-assisted reduction of iron and manganese. In the case of $(\log a_{\text{Ca}^{2+}} + 2\text{pH})$, this parameter could also be decreased by the precipitation of diagenetic calcite, although there was no evidence of this in the Firth of Thames cores. The increase of dissolved silica required to attain the smectite field may be achieved

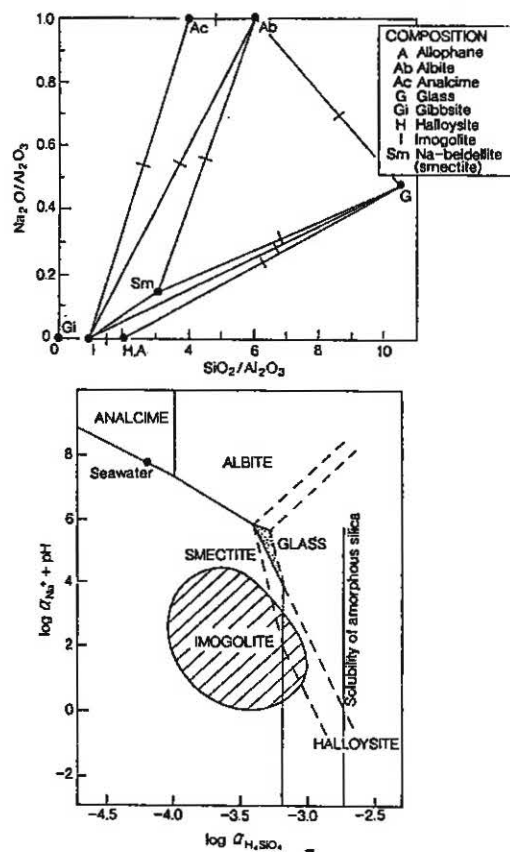


FIG. 2 A. Composition diagram for the $\text{Na}_2\text{O}-\text{SiO}_2-\text{Al}_2\text{O}_3-\text{H}_2\text{O}$ system. Joining lines indicate 'allowed' reactions; the slopes of the phase boundaries are at right angles to these joins. This serves to constrain the topology of the phase boundaries involving glass. The composition diagram assumes idealised compositions of the clay minerals and the composition of glass is taken as that typical of New Zealand rhyolites.
B. Stability diagram: $\log a_{\text{Na}^+} + \text{pH}$ vs $\log a_{\text{H}_4\text{SiO}_4}$. Hatched region is range of soil water compositions from Percival (25). The stability diagram is constructed on the assumption that aluminium is conserved in the system; positions of the stability lines further constrained by the use of standard Gibbs free energy data where available, giving results consistent with Percival (36).

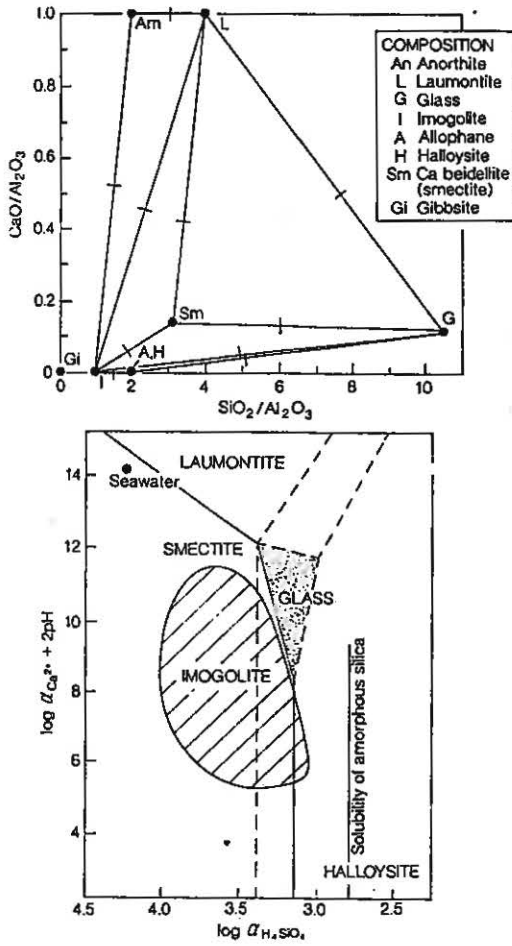


FIG. 3 A. Composition diagram of the CaO-SiO₂-Al₂O₃-H₂O system. The procedure to achieve the stability diagram from this composition diagram is as for Fig. 2.
 B. Stability diagram: log a_{Ca²⁺} + 2pH vs log a_{H₄SiO₄}. Hatched region is range of soil water compositions from Percival (25). The stability diagram is constructed on the assumption that aluminium is conserved in the system; positions of the stability lines further constrained by the use of standard Gibbs free energy data where available, giving results consistent with Percival (36).

during diagenesis (28). An alternative is to consider that although in seawater the formation of imogolite may be thermodynamically favoured, the activation energy for its formation in interstitial waters may be much greater than the activation energy for smectite. Under these conditions smectite might be formed at a rather greater rate than the formation of imogolite. The cores in the Firth of Thames have penetrated the estuarine sediments to a depth of about 5.5 m with a radiocarbon age of ca. 5000 BP at this level. The down-core increasing trend in smectite abundance suggests not only that smectite is forming under these conditions — at the expense of glass (see Fig. 1) — but also that it is forming quickly.

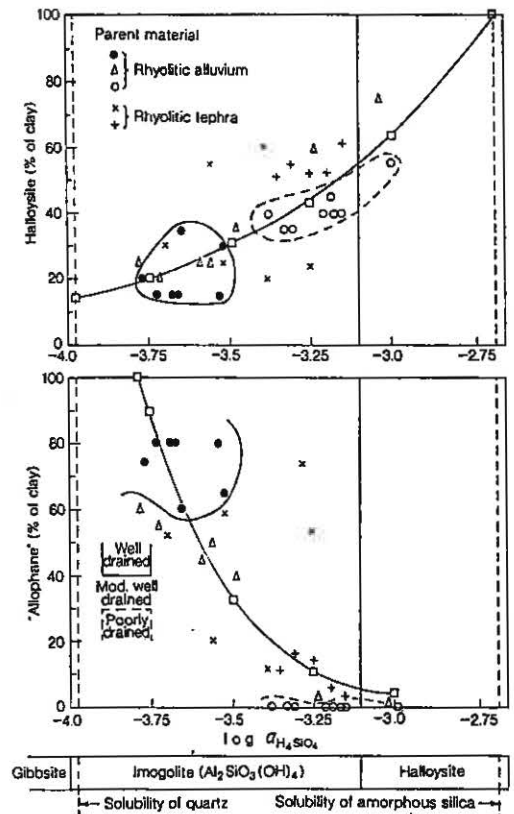


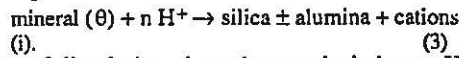
FIG. 4 Halloysitic (A) and 'allophanic' (B) clay mineralogical compositions of soils derived from rhyolitic volcanic materials in northern New Zealand, related to dissolved silica (26).

KINETIC CONTROL ON CLAY MINERAL FORMATION

There have been few studies on the kinetics of clay mineral formation. However, since as is shown later, it is possible to infer the rate of precipitation from dissolution kinetics, it is appropriate to comment briefly on the mechanisms of mineral dissolution.

The solubility of selected silicates and inorganic compounds seems associated with their mechanism for dissolution: more soluble compounds dissolved by transport - or diffusion - controlled mechanisms, those less soluble by surface reaction control (29). Diffusion controlled processes typically have activation energies of about 20 kJ mol⁻¹. Surface reaction control mechanisms may from Fig 5 be inferred to have higher activation energy of dissolution, but these are, nevertheless, generally less than that typical of bond energies. For the clay minerals considered here the values of the equilibrium constant for dissolution, log K, is typically ≤ -10, implying surface reaction control.

For the dissolution of a particular mineral, expressed as:



The rate of dissolution, dependent particularly on pH and temperature, can be expressed (30):

$$\frac{dc_i}{dt} = \frac{A_\theta}{V} v_{i\theta} k_+ (a_{H^+})^{n\theta} \quad (4)$$

where A_θ is the surface area of mineral θ, V is the volume of solution in contact with the mineral θ, v_{iθ} is the stoichiometric content of chemical species i in

mineral θ, n_θ has values in the 0-1 range and k₊ is given by:

$$k_+ = A_+ \exp(-E_+/RT) \quad (5)$$

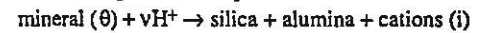
assuming the rate constant k₊ has an Arrhenian temperature dependence, E₊ is an activation energy, A₊ a pre-exponential factor, R the gas constant, and T the temperature. If the dissolution rates do not depend on the concentrations of other components in solution, then (30) as the solution approaches equilibrium equation (4) can be recast as:

$$\frac{dc_i}{dt} = \frac{A_\theta}{V} v_{i\theta} k_+ (a_{H^+})^{n\theta} - \frac{A_\theta}{V} v_{i\theta} \frac{Q_\theta^m}{K_\theta^m} k_+ (a_{H^+})^{n\theta} \quad (6)$$

where m can be any real number, not necessarily an integer, and Q_θ is the reaction activity quotient, and K_θ is the equilibrium constant for dissolution. The second term in equation (6) represents the rate law governing precipitation.

The essence, then, of equation (6) is that the overall rate of a dissolution process can be expressed in terms of thermodynamic parameters associated with that dissolution. More significantly for the present case, the rate of precipitation of a mineral — the second term of equation (6) — is also related to thermodynamic parameters associated with its dissolution.

If a two-step reaction sequence is considered:



then the corresponding expression for (6) is:

$$\frac{dc_i}{dt} = \left\{ \frac{A_\theta}{V} v_{i\theta} k_+ (a_{H^+})^{n\theta} \left(1 - \frac{Q_\theta^m}{K_\theta^m} \right) \right\} - \left\{ \frac{A_\phi}{V} v_{i\phi} k'_+ (a_{H^+})^{p\phi} \left(1 - \frac{Q_\phi^q}{K_\phi^q} \right) \right\} \quad (8)$$

From equation (8) the rate of transformation from glass (θ) to a clay mineral (φ) depends on the equilibrium constants for the dissolution of glass and of clay minerals and their respective reaction activity coefficients. These coefficients can be calculated from the concentrations of the appropriate chemical species in soil and interstitial waters that host the reactions (see Table 1)

As a first step to determining whether the dissolution of silica-bearing glass or the formation of the clay mineral is rate determining, if it is assumed that:

$$A_\theta = A_\phi = A; v_\theta = \rho\phi = 1; v_\rho = 1 \quad (9)$$

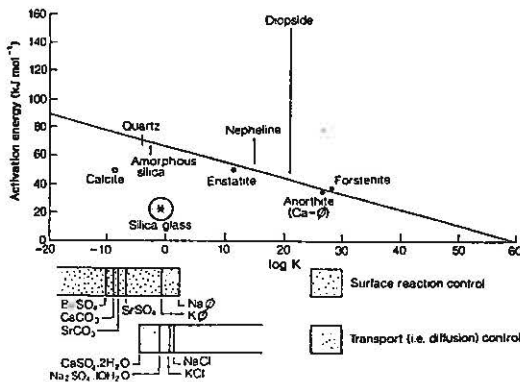


FIG. 5 Relationship between activation energy for dissolution of minerals and their equilibrium constants for dissolution (30) Also shown is the inferred mechanism for dissolution (29)

TABLE 1: Clay mineral dissolution data

MINERAL	
(pH-range)	Reaction
log K_{ϕ}	log Q_{ϕ}
IMOGOLITE	
(basic)	$\text{Al}_2\text{SiO}_3(\text{OH})_4 + 5\text{H}_2\text{O} \rightarrow 2\text{Al}(\text{OH})_4^- + \text{H}_4\text{SiO}_4 + 2\text{H}^+$
log $K_I = -36.04$	log $Q_I = \log^a \text{H}_4\text{SiO}_4 + 2 \log^a \text{Al}(\text{aq}) - 2\text{pH}$
(neutral)	$\text{Al}_2\text{SiO}_3(\text{OH})_4 + \text{H}_2\text{O} + 2\text{H}^+ \rightarrow 2\text{Al}(\text{OH})_2^+ + \text{H}_4\text{SiO}_4$
log $K_I = -9.38$	log $Q_I = 2 \log^a \text{Al}(\text{aq}) + \log^a \text{H}_4\text{SiO}_4 + 2\text{pH}$
(acid)	$\text{Al}_2\text{Si}_2\text{O}_3(\text{OH})_4 + 6\text{H}^+ \rightarrow 2\text{Al}^{3+} + \text{H}_4\text{SiO}_4 + 3\text{H}_2\text{O}$
log $K_I = +10.08$	log $Q_I = 2 \log^a \text{Al}(\text{aq}) + \log^a \text{H}_4\text{SiO}_4 + 6\text{pH}$
HALLOYSITE	
(basic)	$\text{Al}_2\text{Si}_2\text{O}_5(\text{OH})_4 + 7\text{H}_2\text{O} \rightarrow 2\text{Al}(\text{OH})_4^- + 2\text{H}_4\text{SiO}_4 + 2\text{H}^+$
log $K_H = -38.6$	log $Q_H = 2 \log^a \text{Al}(\text{aq}) + 2 \log^a \text{H}_4\text{SiO}_4 - 2\text{pH}$
(neutral)	$\text{Al}_2\text{Si}_2\text{O}_5(\text{OH})_4 + 3\text{H}_2\text{O} + 2\text{H}^+ \rightarrow 2\text{Al}(\text{OH})_2^+ + 2\text{H}_4\text{SiO}_4$
log $K_H = -11.94$	log $Q_H = 2 \log^a \text{Al}(\text{aq}) + 2 \log^a \text{H}_4\text{SiO}_4 + 2\text{pH}$
(acid)	$\text{Al}_2\text{Si}_2\text{O}_5(\text{OH})_4 + 6\text{H}^+ \rightarrow 2\text{Al}^{3+} + 2\text{H}_4\text{SiO}_4 + \text{H}_2\text{O}$
log $K_H = +7.54$	log $Q_H = 2 \log^a \text{Al}(\text{aq}) + 2 \log^a \text{H}_4\text{SiO}_4 + 6\text{pH}$
Na - SMECTITE	
(basic)	$\text{Na}_{0.33}\text{Al}_{2.33}\text{Si}_{3.67}\text{O}_{10}(\text{OH})_2 + 12\text{H}_2\text{O} \rightarrow 0.33\text{Na}^+ + 2.33 \text{Al}(\text{OH})_4^- + 3.67 \text{H}_4\text{SiO}_4 + 2\text{H}^+$
log $K_S = -47.5$	log $Q_S = 0.33 \log^a \text{Na}^+ + 2.33 \log^a \text{Al}(\text{aq}) + 3.67 \log^a \text{H}_4\text{SiO}_4 - 2\text{pH}$

Table 1.contd.

(neutral)	$\text{Na}_{0.33}\text{Al}_{2.33}\text{Si}_{3.67}\text{O}_{10}(\text{OH})_2 + 7.33\text{H}_2\text{O} + 2.66\text{H}^+ \rightarrow 0.33\text{Na}^+ + 3.67\text{H}_4\text{SiO}_4 + 2.33\text{Al}(\text{OH})_2^+$
$\log K_S = -16.05$ 2.66pH	$\log Q_S = 0.33 \log^a \text{Na}^+ + 2.33 \log^a \text{Al}(\text{aq}) + 3.67 \log^a \text{H}_4\text{SiO}_4 - 2.66\text{pH}$
(acid)	$\text{Na}_{0.33}\text{Al}_{2.33}\text{Si}_{3.67}\text{O}_{10}(\text{OH})_2 + 7.33\text{H}^+ + 2.68\text{H}_2\text{O} \rightarrow 0.33\text{Na}^+ + 3.67\text{H}_4\text{SiO}_4 + 2.33\text{Al}^{3+}$
$\log K_S = -8.48$ $+7.33\text{pH}$	$\log Q_S = 0.33 \log^a \text{Na}^+ + 2.33 \log^a \text{Al}(\text{aq}) + 3.67 \log^a \text{H}_4\text{SiO}_4 + 7.33\text{pH}$

SILICA GLASS

--	$\text{SiO}_2 + 2\text{H}_2\text{O} \rightarrow \text{H}_4\text{SiO}_4$
$\log K_\theta = -1.454$	$\log Q_\theta = \log^a \text{H}_4\text{SiO}_4$

then equation (8) reduces to:

$$d c_i / dt = \left(\frac{A}{V} a_{\text{H}^+} \right) [k_+ (1 - Q_\theta / K_\theta) - k'_+ (1 - Q_\phi / K_\phi)] \quad (10)$$

Although the activation energy for diffusion in glass is generally cited as 20 kJ mol^{-1} , activation energies for process involving silica loss from glass are inferred to be higher (see Fig 5, $\sim 60 \text{ kJ mol}^{-1}$). Data obtained under hydrothermal conditions (31) yielded an activation energy of 54 kJ mol^{-1} . Assuming an Arrhenian temperature dependence of rate constant, these same data give a rate constant (k_+) of $2.2 \times 10^{-7} \text{ s}^{-1}$ when extrapolated to 25°C . For the dissolution of kaolinite a rate constant of $1.24 \times 10^{-12} \text{ mol m}^{-2} \text{ s}^{-1}$ at a pH of 3 and at 80°C is recorded (32). From the empirical relationship of Fig 5:

$$E_+ = -1.125 \log K + 68 \quad (E_+ \text{ in } \text{kJ mol}^{-1}) \quad (11)$$

the activation energy for the dissolution of kaolinite is calculated as 83 kJ mol^{-1} . Assuming an Arrhenian temperature dependence for this reaction, the rate constant at 25°C is determined as

$6.7 \times 10^{-7} \text{ mol m}^{-2} \text{ s}^{-1}$, whence equation (10) reduces to

$$d c_i / dt = \left(\frac{A}{V} a_{\text{H}^+} \right) [2.2 \times 10^{-7} (1 - Q_\theta / K_\theta) - 6.7 \times 10^{-15} (1 - Q_\phi / K_\phi)] \quad (12)$$

In most interstitial and soil waters (see Tables 2-4), a reasonable approximation is

$$(1 - Q_\phi / K_\phi) = 1 \quad (13)$$

whence equation (12) becomes:

$$d c_i / dt = \left(\frac{A}{V} a_{\text{H}^+} \right) [2.2 \times 10^{-7} + 6.7 \times 10^{-15} (Q_\theta / K_\theta - 1)] \quad (14)$$

For the formation of the clay mineral kaolinite to have a comparable effect on the overall rate of its formation as the dissolution of glass, the reaction activity coefficient must be such that

$$\log (Q_\phi / K_\phi) > 7.5 \quad (15)$$

Thus, an indicator of the likelihood of the formation of a given clay mineral being rate determining can be estimated from the parameter $\log (Q_\phi / K_\phi)$, or from the parameter R_ϕ where

$$R_\phi = 2.3 \times 10^{-7} (1 - Q_\theta / K_\theta) - 6.7 \times 10^{-15} (1 - Q_\phi / K_\phi) \quad (16)$$

This is done in the next section for the formation of imogolite, halloysite, and smectite under estuarine and inferred shallow marine diagenetic conditions and also in soil waters associated with rhyolitic tephra.

The chemical reaction and the equilibrium constants ($\log K_\phi$) for the dissolution of the clay minerals imogolite, halloysite, and smectite, together

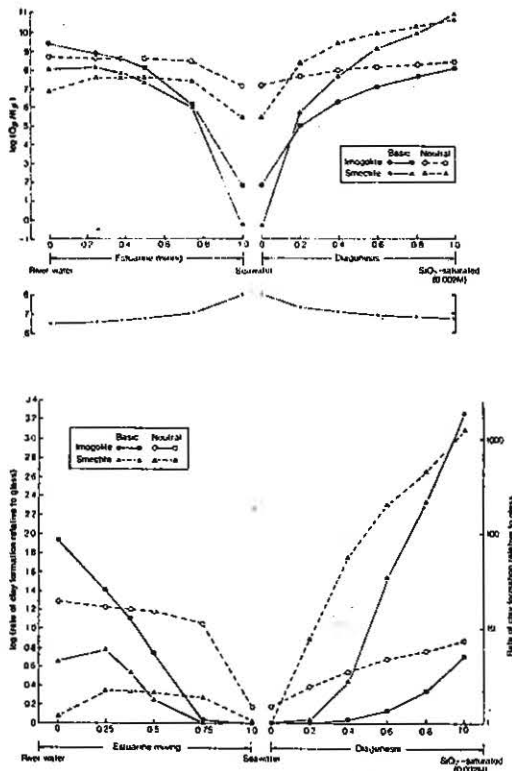


FIG. 6 Inferred precipitation rate of imogolite and smectite in estuarine and interstitial waters in marine sediments.

- A. the parameter $\log(Q\phi/K\phi)$ vs mixing extent.
 B. the parameter $R\phi$ vs mixing extent.

with expressions for their reaction activity coefficients ($\log Q\phi$) are given in Table 1. In these expressions and calculations it is assumed that the dominant aluminium species in basic solution is $Al(OH)_4^-$, in near neutral solution $Al(OH)_2^+$, and in acid solution Al^{3+} . Also shown on Table 1 are the corresponding parameters ($\log K\phi$, $\log Q\phi$) for the dissolution of silica glass.

To use this approach to predict the likely rate of clay mineral formation the concentration of dissolved species in estuarine waters, interstitial waters in marine sediments, and soil waters are required. If estuarine waters are assumed to be a mixture of average river water (23) and seawater, with all components mixed in

equal proportions, and if interstitial waters are taken to range from seawater to a solution wherein the solution is saturated with respect to amorphous silica, values of the parameters $Q\phi/K\phi$ for glass $Q\phi/K\phi$ for clay minerals and the derived parameter $R\phi$ for the clay minerals can be calculated. The results of these calculations are shown in Table 2 and plotted in Fig. 6. Although the plot Fig. 6B shows more dramatically that smectite is formed rapidly than imogolite once the concentration of silica starts to increase (i.e., with diagenesis), the trend is also apparent on Fig. 6A, where there is no particular assumption about the relative rate constants for dissolution (viz, k_+ , k_+).

Similar calculations for the formation of smectite, halloysite, and imogolite in a free-draining soil formed from rhyolitic tephra show that the rate of formation of imogolite far exceeds that of smectite and is slightly higher than that for halloysite (Table 3). Comparison of the rate proxies ($R\phi$) between Tables 2 and 3 indicate that the rate of formation of smectite during early diagenesis may be orders of magnitude higher than the rate of formation of imogolite in soil water. For a soil with impeded drainage the rates of formation of halloysite and imogolite seem similar, but in the lower horizons there seems little difference between these rates and those inferred for the dissolution of glass (Table 4). There seems a sympathetic relationship between the relative rate of formation of halloysite and imogolite and the actual proportions of each of halloysite and allophane in soils (Fig. 7). This suggests that the formation of the clay minerals in these soils is more a consequence of kinetics than thermodynamic stability. The inferred similar rate to that of glass dissolution may also suggest that the clay-mineral forming processes in soil are diffusively controlled rather than surface reaction controlled.

MECHANISTIC IMPLICATIONS

As noted by Lasaga (30) and shown on Fig. 5, activation energies of the dissolution of clay minerals are generally higher than those typical for transport in solution ($\sim 20 \text{ kJ mol}^{-1}$), but less than that expected for the breaks of bonds ($160 - 400 \text{ kJ mol}^{-1}$). The equilibrium constants for halloysite and imogolite dissolution under acid conditions — as in the C-horizon of the poorly drained tephra derived soil — are rather higher (7.54 and 10.08, respectively). On the basis of Fig. 5, these processes could be diffusively controlled with activation energies of 60 and 57 kJ mol^{-1} respectively.

Jambon (33) derived a relationship between the activation energy for diffusion (E^*) in obsidian and the radius (r) and charge (z) of the diffusing ions, viz.

$$E^* = 4.184 [8 + 128(r - 1.34)^2 + 33 z^2/(r + 1.34)] \quad (17)$$

In this expression r is the radius of the ion, in

TABLE 2. Inferred rates of clay mineral formation in estuarine and intertidal waters in nearshore marine sediments

	Soil horizon (1)									
	0	0.25	0.50	0.75	1.0	1.5	2.0	2.5	3.0	3.5
Water characteristics										
pH	8.5	8.42	8.09	8.71	7.02	8.0	7.22	7.07	8.22	8.00
log aNa ⁺	-3.64	-0.73	-0.73	-0.62	-0.46	-0.33	0.35	0.90	0.75	0.85
log aH ₂ SiO ₄	-3.76	-3.81	-3.85	-3.86	-3.32	-3.98	-3.56	-3.55	-3.93	-3.83
log aAl(OH) ₃	-3.92	-6.05	-5.12	-5.22	-5.22	-7.20	-4.82	-4.27	-6.12	-5.81
GLASS log (C ₀ /K ₀)	-2.31	-2.36	-2.38	-2.41	-2.47	-2.53	-1.85	-1.80	-1.45	-1.24
IMC... JITE log(Q ₁ /K ₁) (based on R ₁)	3.44	8.39	8.59	8.16	8.18	1.86	5.08	6.31	7.08	8.14
IMOGOLITE log(Q ₁ /K ₁) (based on R ₁)	19.5	8.71	8.89	8.06	8.54	7.20	7.64	7.33	8.08	8.18
HALLOYSITE log(Q ₁ /K ₁) (based on R ₁)	8.06	3.25	7.50	7.43	8.64	-0.03	8.70	7.78	8.03	8.85
log(Q ₁ H/K ₁) - log(Q ₂ /K ₂) ⁽⁵⁾	8.23	6.07	3.42	7.77	1.00	1.00	1.01	2.90	34.8	267
GLASS log (C ₀ /K ₀)	5.88	7.60	7.81	7.57	7.47	5.48	8.34	9.26	9.00	10.2
% allophane of soil (6)	12.5	13.0	12.3	10.0	10.4	17.8	18.0	13.8		

(1) from Drever, 1982, table 10-2
 (2) calculated concentrations, assuming all components mixed in same proportion
 (3) Water saturated with respect to amorphous silica
 (4) Al (aq) is the aluminum observed in the water, being principally Al(OH)₃ under basic pH conditions and Al(OH)₂⁺ in near neutral pH conditions.
 (5) R₁ the proxy for rate, calculated as (G-C)/G where G=2.2*10⁻⁷ (1-Q₁/K₁) and C=6.7*10⁻¹⁵(1-Q₁/K₁)⁴ where φ = 3, 1

TABLE 3. Inferred rate of clay mineral formation in soil waters in a well drained soil profile developed on rhyolite tephra

	Soil horizon (1)							
	AW1	AW2	B/A	BW1	BW2	BW3	2Cg	C
	Depth below surface (cm)							
	0-8	6-17	17-31	31-55	55-73	73-81	81-107	107-130
WATER CHARACTERISTICS (1)								
pH	5.3	4.98	5.50	6.85	7.05	6.80	6.70	6.30
log aNa ⁺	-3.66	-3.14	-3.32	-3.29	-3.44	-3.51	-3.49	-3.38
log aH ₂ SiO ₄	-4.77	-5.13	-5.72	-5.82	-5.86	-5.88	-5.72	-5.15
log aAl(OH) ₃	-4.77	-5.13	-5.72	-5.82	-5.86	-5.88	-5.72	-5.15
GLASS log (C ₀ /K ₀)	-2.21	-2.07	-2.08	-2.29	-2.23	-2.23	-2.25	-2.25
SMECTITE log (Q ₁ /K ₁) ⁽²⁾	4.38	3.31	3.30	5.89	6.27	5.58	5.59	3.89
IMOGOLITE log (Q ₁ /K ₁) (R ₁) ⁽⁴⁾	6.78	5.50	5.41	7.70	7.88	7.38	7.80	5.98
HALLOYSITE log(Q ₁ /K ₁) (R ₁)	1.18	1.01	1.06	2.54	3.30	1.74	2.22	1.03
log(Q ₁ H/K ₁) - log(Q ₂ /K ₂) ⁽⁵⁾	5.38	4.54	4.48	8.52	8.78	8.28	8.42	4.04
R ₁ /R ₂	1.02	1.00	1.00	1.10	1.17	1.08	1.08	1.00
log(Q ₁ H/K ₁) - log(Q ₂ /K ₂) ⁽⁵⁾	0.86	1.01	1.02	0.43	0.35	0.61	0.49	0.97
	-1.10	-0.98	-0.93	-1.18	-1.12	-1.12	-1.18	-1.14
% allophane of soil (6)	10.8	10.4	12.8	22.4	14.9	26.4	6.0	
% halloysite of soil (6)	6.3	4.8	2.4	4.2	2.7	5.0	1.6	

(1) Horotiu silt loam is a well drained yellow loam (umbric vitrandept) sampled at Ruakura near Hamilton, North Island, New Zealand.
 (2) from Percival (1966)
 (3) as these values are small relative to log (Q₁/K₁), φ = 1, H, they are not considered further
 (4) R₁ is the proxy for rate, calculated as (G-C)/G where G=2.2*10⁻⁷(1-Q₁/K₁) and C=6.7*10⁻¹⁵(1-Q₁/K₁)⁴ where φ = H, 1
 (5) This is akin to the ratio R₁/R₂ but makes no assumption about k₁, k₂ (see text)
 (6) from Singleton et al. (1989)

VIII - fold co-ordination in A^o (34) and E* has units of kJ mol⁻¹. Jambon noted, however, that the activation energy is lower where the glass contains water. On the basis of the decreases in activation energy he noted for Cs (209 to 84 kJ mol⁻¹), Na (84 to 67 kJ mol⁻¹) and Ca

TABLE 4. Inferred rate of clay mineral formation in soil waters in a poorly drained soil profile developed on rhyolite tephra

	Soil horizon (1)							
	AW1	A/B	B/A	Brg1	Brg2	2Brg2	2Brg2	3Cr
	Depth below surface (cm)							
	0-9	9-22	22-32	32-39	39-57	57-70	70-80	80-83
WATER CHARACTERISTICS (1)								
pH	6.65	6.10	6.35	5.80	5.30	5.25	4.95	4.80
log aNa ⁺	-2.96	-2.98	-3.13	-3.09	-2.97	-3.14	-3.12	-3.11
log aH ₂ SiO ₄	-3.34	-3.31	-3.38	-3.21	-3.17	-3.19	-3.17	-3.00
log aAl(OH) ₃	-5.72	-5.38	-5.15	-5.82	-5.72	-5.68	-5.59	-5.09
GLASS log (C ₀ /K ₀)	-1.89	-1.88	-1.93	-1.78	-1.72	-1.74	-1.72	-1.55
SMECTITE log (Q ₁ /K ₁) ⁽²⁾	7.17	6.86	7.51	5.12	4.21	4.00	3.54	5.06
IMOGOLITE log (Q ₁ /K ₁) (R ₁) ⁽⁴⁾	7.9	7.55	8.4	6.13	5.37	5.37	4.93	5.54
HALLOYSITE log(Q ₁ /K ₁) (R ₁)	3.45	2.10	8.7	1.0	1.0	1.0	1.0	1.0
log(Q ₁ H/K ₁) - log(Q ₂ /K ₂) ⁽⁵⁾	7.10	6.80	7.58	5.48	4.78	4.74	4.32	5.08
R ₁ /R ₂	1.39	1.19	2.15	1.0	1.0	1.0	1.0	1.0
log(Q ₁ H/K ₁) - log(Q ₂ /K ₂) ⁽⁵⁾	0.40	0.57	0.25	1.0	1.0	1.0	1.0	1.0
	-0.8	-0.75	-0.82	-0.65	-0.61	-0.63	-0.61	-0.46
% allophane of soil (6)	0	0	0	0	0	0	0	0
% halloysite of soil (6)	12.5	13.0	12.3	10.0	10.4	17.8	18.0	13.8

(1) Te Kowhai silt loam is a poorly drained grey soil (typic ochraqualis) sampled at Ruakura near Hamilton, North Island, New Zealand
 (2) from Percival (1966)
 (3) as these values are small compared to log (Q₁/K₁), φ = H, 1, they are not considered further
 (4) R₁ is the proxy for rate, calculated as (G-C)/G where G=2.2*10⁻⁷(1-Q₁/K₁) and C=6.7*10⁻¹⁵(1-Q₁/K₁)⁴ where φ = 4, 1
 (5) This is akin to the ratio R₁/R₂ but makes no assumption about k₁, k₂ (see text)
 (6) from Singleton et al. (1989)

TABLE 5: Calculated activation energies for the diffusion of selected cations in glass

Ion	charge	activation energy ⁽²⁾	radius ⁽¹⁾	
			r [VIII] (A ^o)	E* (kJ mol ⁻¹)
	Z			
Al ³⁺	3	0.74(3)		220
Al(OH) ₂ ⁺	1	1.73		77
Al(OH) ₃ ⁰	0	1.97		88
Al(OH) ₄ ⁻	1	2.15		120
Si ⁴⁺	4	0.48(3)		392
H ₄ SiO ₄ ⁰	0	2.13		110

(1) from Wittaker and Muntus (34), as used by Jambon (32)
 (2) equation (18)
 (3) extrapolated from radii at lower co-ordination numbers

- California Obsidian Studies*. Berkley Department of Anthropology, University of California, Berkley
10. White, A.F. and Claassen, H.C. (1980). Kinetic model for the short-term dissolution of a rhyolitic glass. *Chemical Geology*, **28**, 91-109.
 11. White, A.F. (1983). Surface chemistry and dissolution kinetics of glassy rocks at 25°C. *Geochimica et Cosmochimica Acta*, **47**, 805-815.
 12. Hodder, A.P.W. (1985). Effects of composition on hydration kinetics in volcanic glasses: implications for dating. *Journal of Colloid and Interface Science*, **103**, 45-49.
 13. Hodder, A.P.W., Green, B.E. and Lowe, D.J. (1990). A two-stage model for the formation of clay minerals from tephra-derived volcanic glass. *Clay Minerals*, **25**, 313-327.
 14. Ross, C.S. and Shannon, E.V. (1926). Minerals of bentonite and related clays and their physical properties. *Journal of the American Ceramic Society*, **9**, 77-96.
 15. Peterson, M.N.A. and Griffin, J.J. (1964). Volcanism and clay minerals in the southeastern Pacific. *Journal of Marine Research*, **22**, 287-312.
 16. Hein, J.R. and Scholl, D.W. (1978). Diagenesis and distribution of late Cenozoic volcanic sediment in the South Bering Sea. *Geological Society of America Bulletin*, **89**, 197-210.
 17. Hein, J.R., Scholl, D.W. and Miller, J. (1978). Episodes of Aleutian Ridge explosive volcanism. *Science*, **199**, 137-141.
 18. Gardner, J.V., Nelson, C.S. and Baker, P.A. (1986). Distribution and character of pale green laminae in sediment from Lord Howe Rise: a probable late Neogene and Quaternary tephrostratigraphic record. *Initial Reports of the Deep Sea Drilling Project*, **90**, 1145-1159.
 19. Chamley, H. (1990). *Clay Sedimentology*. Springer, Berlin. 623pp.
 20. Millot, G. (1970). *Geology of Clays*. Springer, Berlin, 425pp.
 21. Naish, T.R., Nelson, C.S. and Hodder, A.P.W. (1993). Evolution of Holocene sedimentary bentonite in a shallow marine embayment, Firth of Thames, New Zealand. *Marine Geology*, **109**, 267-278.
 22. Hodder, A.P.W., Naish, T.R. and Nelson, C.S. (1993). A two-stage model for the formation of smectite from detrital volcanic glass under shallow marine conditions. *Marine Geology*, **109**, 279-285.
 23. Drever, J.I. (1982). *The Geochemistry of Natural Waters*. Prentice-Hall, Englewood Cliffs.
 24. Percival, H.J. (1985). Soil solutions, minerals, and equilibria. *New Zealand Soil Bureau Report*, 69.
 25. Percival, H.J. (1986). Data In: Joe, E.N. (comp.), Soil water characterisation studies of six soils in the Waikato district, New Zealand. *New Zealand Soil Bureau SWAMP Data Sheets 1984*, 1-6, New Zealand Department of Scientific and Industrial Research, Lower Hutt.
 26. Singleton, P.L., McLeod, M. and Percival, H.J. (1989). Allophane and halloysite content and soil solution silicon in soils from rhyolitic volcanic material, New Zealand. *Australian Journal of Soil Research*, **27**, 67-77.
 27. Burdige, D.J. (1994). The biogeochemistry of manganese and iron reduction in marine sediments. *Earth Science Reviews*, **35**, 249-284.
 28. Sholkovitz, E. (1973). Interstitial water chemistry of the Santa Barbara Basin Sediments. *Geochimica et Cosmochimica Acta*, **37**, 2043-2073.
 29. Berner, R.A. (1980). *Early Diagenesis: a Theoretical Approach*. Princeton University Press, Princeton.
 30. Lasaga, A.C. (1984). Chemical kinetics of water-rock interactions. *Journal of Geophysical Research*, **89**, 4009-4025.
 31. Hawkins, D.B. (1981). Kinetics of glass dissolution and zeolite formation under hydrothermal conditions. *Clays and Clay Minerals*, **29**, 331-339.
 32. Nagy, K.L., Blum, A.E. and Lasaga, A.C. (1991). Dissolution and precipitation kinetics of kaolinite at 80°C and pH3: the dependence on solution saturation state. *American Journal of Science*, **291**, 649-686.
 33. Jambon, A. (1982). Tracer diffusion in granitic melts: experimental results for Na, K, Rb, Cs, Ca, Sr, Ba, Ce, Eu to 1300°C and a model of calculation. *Journal of Geophysical Research*, **87**, 10797-10810.
 34. Wittaker, E.J.W. and Muntus, R. (1970). Ionic radii for use in geochemistry. *Geochimica et Cosmochimica Acta*, **34**, 945-956.
 35. Childs, C.W., Parfitt, R.L. and Newman, R.H. (1990). Structural studies of Silica Springs allophane. *Clay Minerals*, **25**, 329-341.
 36. Percival, H.J. (1995). Relative stabilities of selected clay minerals in soils based on a critical selection of solubility constants. *Proceedings 10th International Clay Conference*, (Adelaide). CSIRO Publications, Melbourne (in press)